Supporting Information for

GTP State-Selective Cyclic Peptides Ligands of K-Ras(G12D) Block its Interaction with Raf

Ziyang Zhang[1,3], Rong Gao[2,3], Qi Hu[1], Hayden Peacock[2], D. Matthew Peacock[1], Shizhong Dai[1], Kevan M. Shokat[1*], Hiroaki Suga[2*]

[1]Department of Cellular and Molecular Pharmacology, Howard Hughes Medical Institute, University of California-San Francisco, California 94158, USA

[2]Department of Chemistry, Graduate School of Science, The University of Tokyo, 7-3-1 Bunkyo-ku, Tokyo 113-0033, Japan

[3]These authors contributed equally to this work.

*Correspondence: kevan.shokat@ucsf.edu (K.M.S.), hsuga@chem.s.u-tokyo.ac.jp (H.S.)

Table of Contents

Supplementary Figures and Tables 4

Figure S1. (Related to Figure 1). A separate screen using K-Ras(G12D/T35S)•GppNHp as positive selection target and empty beads as negative selection target 4

Figure S2. Biophysical characterization of cyclic peptides binding to K-Ras(G12D). 5

Figure S3. Thermal denaturation experiments reveal that KD1, KD2, and KD17 do not increase the melting temperature of K-Ras (G12D) 6

Figure S4. HSQC spectra of apo, KD2-bound, and KD17-bound K-Ras(G12D)•GppNHp showing global chemical shift perturbation upon ligand binding 7

Figure S5. (Related to Figure 3). Additional views of the KD2•KRas(G12D)•GppNHp cocrystal structure. 8

Figure S6. Cellular activity of cyclic peptides. 9

Figure S7. Cell permeability of cyclic peptides. 10

Figure S8. A KD2-Thalidomide derivative failed to induce Ras degradation 11

Table S1. Data collection and refinement statistics 12

Additional Discussion on the Cellular Activity of Cyclic Peptides 13

Safety Notes 14

Cyclic Peptide Selection 14

Selection 14

Comparison selection 15

Cyclic Peptide Synthesis 15

General Workflow 15

Resin preparation 16

Amino Acid Coupling 16

N-terminal capping with chloroacetamide 16

Deprotection and Cleavage 17

Cyclization 17

Synthesis of C-terminally Modified Cyclic Peptides (ct-KD2 and KD2-thalidomide) 18

Synthesis of Thr10 variants of KD2 18

Protein Expression and Purification 18

K-Ras(G12D) CysLight 18

Biotinylated K-Ras Proteins 18

GST-Raf1-RBD and Sos^{cat} 19

Other Proteins 20

Cell Culture 20
Gel Electrophoresis and Western Blot 20
Biolayer Interferometry 20
Surface Plasmon Resonance 21
Isothermal Titration Calorimetry 22
Differential Scanning Fluorimetry 22
Sos- or EDTA-mediated Nucleotide Exchange Assay 22
Time-Resolved Fluorescence Resonance Energy Transfer (TR-FRET) Assay 23
Chloroalkane Cell Penetration (CAPA) Assay 23
Passive Artificial Membrane Permeability Assay (PAMPA) 24
Caco-2 Monolayer Permeability Assay 24
Crystallization 24
X-Ray Data Collection and Structure Determination 25
Heteronuclear Single-Quantum Coherence (HSQC) 25
Materials 25
List of Antibodies 26
List of Buffer Composition 26
List of Protein Sequences Used in This Study 27
Characterization Data for Cyclic Peptides 29
Mass Spectrometry 29
UPLC Analysis 29
References 31

Supplementary Figures and Tables

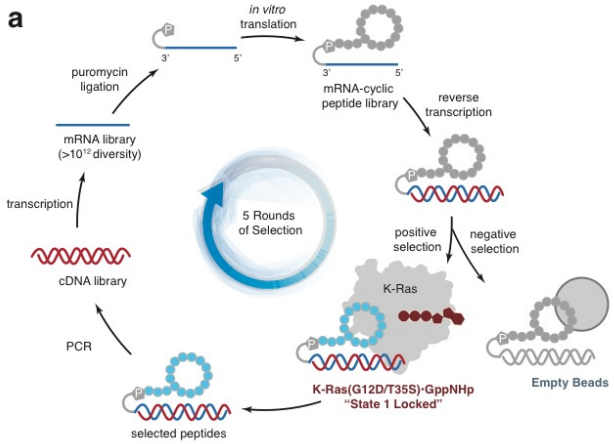

b

Ranking	Peptide Backbone	Linker	Length	GppNHp /GDP	GppNHp /Beads
1	**DYC - - - - PFTWLTCLYKC**	**GSGSGS**	**19**	**0.21**	**483**
4	DYC - - - - PLTWLTCLYKC	GSGSGS	19	0.30	926
8	DYC - - - - PFTWLTCLYKC	GSSSGS	19	0.23	593
6	DYC - - - - PFTWLTCLYKC	SSGSGS	19	0.24	650
11	DYC - - - - PFTWLTCLYKC	GSGSSS	19	0.22	527
12	DYC - - - - PFTWLTCLYKC	GSGSAA	19	0.22	497
13	DYC - - - - PFTWLTCLYRC	GSGSGS	19	0.22	486
17	DYC - - - - PFTWLTCLYKC	GSGGGS	19	0.20	392
18	DYF - - - - PFTWLTCLYKC	GSGSGS	19	0.20	446
19	DYC - - - - PFTWLTCLYKC	GGGSGS	19	0.21	377
2	**DYIIVTEKFIWV - - - HHC**	**GSGSGS**	**20**	**3.95**	**796**
3	**DYSW - KWPIFYKGP - - - C**	**GSGSGS**	**19**	**0.58**	**878**
14	DYSW - KWPIFYKGP - - - C	GSGSSS	19	0.67	970
7	**DYVW - - - PIFC - GPTLC**	**GSGSGS**	**19**	**0.44**	**207**
16	DYVW - - - PIFC - GPTLC	RGSGSGS	19	0.48	515
5	**DYCILFTRWDW - - - - PCC**	**GSGSGS**	**19**	**0.52**	**288**
15	DYCILFTRWDW - - - - PCC	GSSSGS	19	0.54	329
9	**DYCIMFVSHD - - - - - QCC**	**GSGSGS**	**18**	**0.71**	**592**
10	DYCIIKTRLDY - - - - CCC	GSGSGS	19	0.45	320
20	**DYFVNFRNFRT - - - - FRC**	**GSGSGS**	**19**	**10.31**	**220**
Concensus	DYC - - - - PFTWLTCLYKC	GSGSGS	–	–	–

Figure S1. (Related to Figure 1). A separate screen using K-Ras(G12D/T35S)•GppNHp as positive selection target and empty beads as negative selection target (a) led to primarily GDP-state selective binders of K-Ras (b). Note that some of the hits do overlap with the results in the primary screen: peptide 2 is identical to KD1, and peptide 20 is identical to KD2.

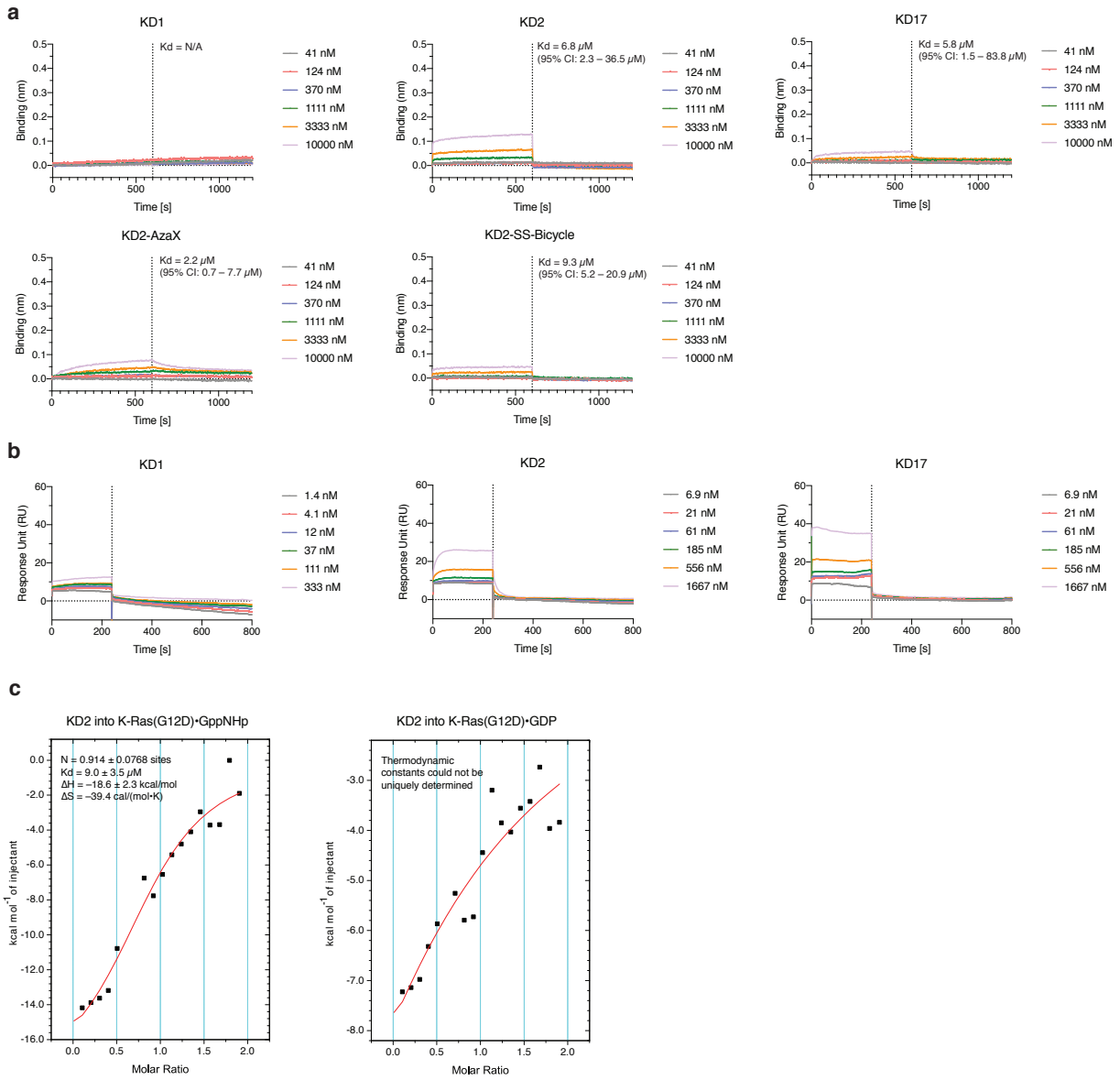

Figure S2. Biophysical characterization of cyclic peptides binding to K-Ras(G12D). **a**, measurement of the binding of KD1, KD2, KD17, KD2-AzaX, KD2-SS-Bicycle to surface-immobilized K-Ras(G12D)•GppNHp using biolayer interferometry. Signal was obtained with double reference to empty sensors and DMSO controls. Saturation binding could not be achieved due to solubility limitations. Dissociation constants (Kd) were determined by fitting steady-state response against peptide concentration to a one-site binding model. **b**, measurement of the binding of KD1, KD2, and KD17 to surface-immobilized K-Ras(G12D)•GppNHp using surface plasmon resonance. **c**, measurement of the binding of KD2 to K-Ras(G12D)•GppNHp using isothermal titration calorimetry (ITC). Thermodynamic constants were determined by fitting the curve to a one-site binding model.

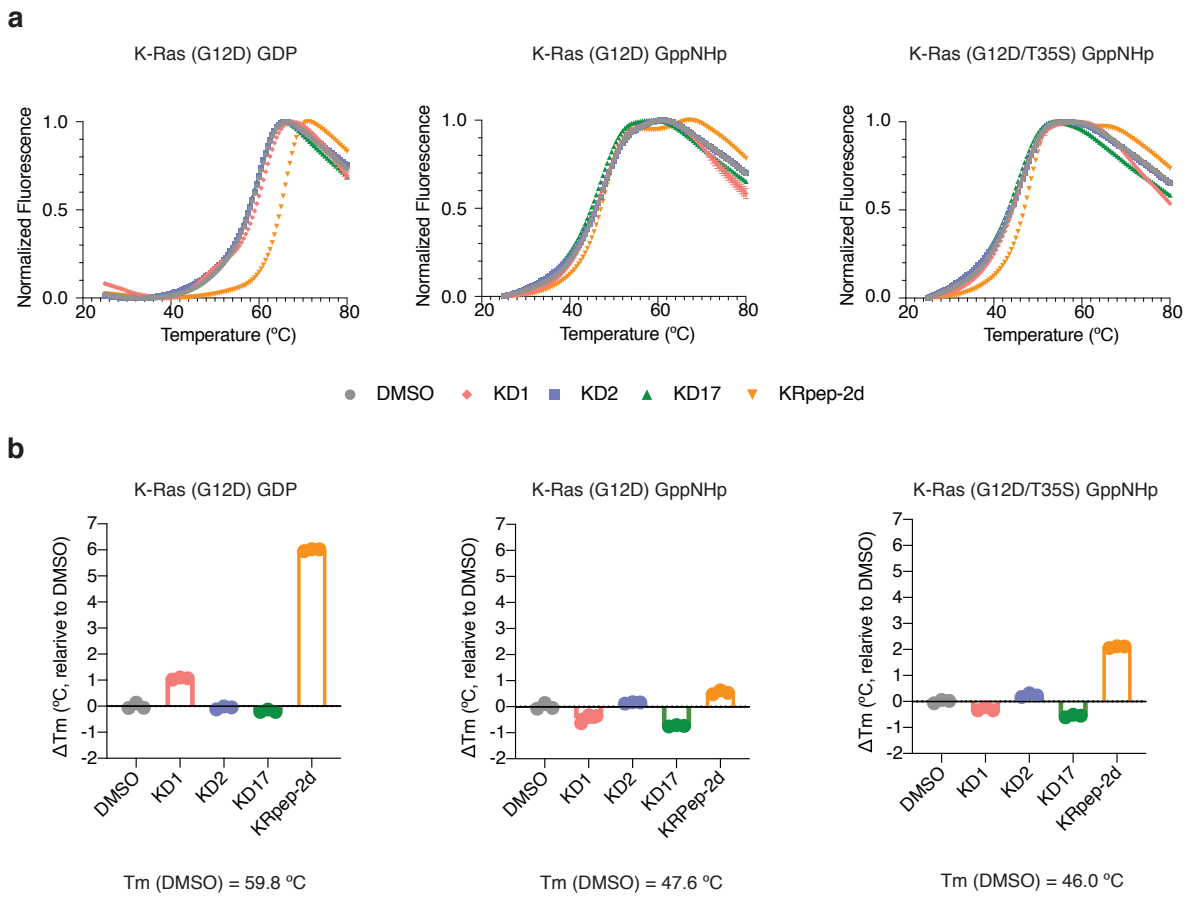

Figure S3. Thermal denaturation experiments reveal that KD1, KD2, and KD17 do not increase the melting temperature of K-Ras (G12D). a, differential scanning fluorimetry curves of K-Ras(G12D)•GDP, K-Ras(G12D)•GppNHp, K-Ras(G12D/T35S)•GppNHp in the presence of cyclic peptides. **b**, changes of protein melting temperature for experiments in (a).

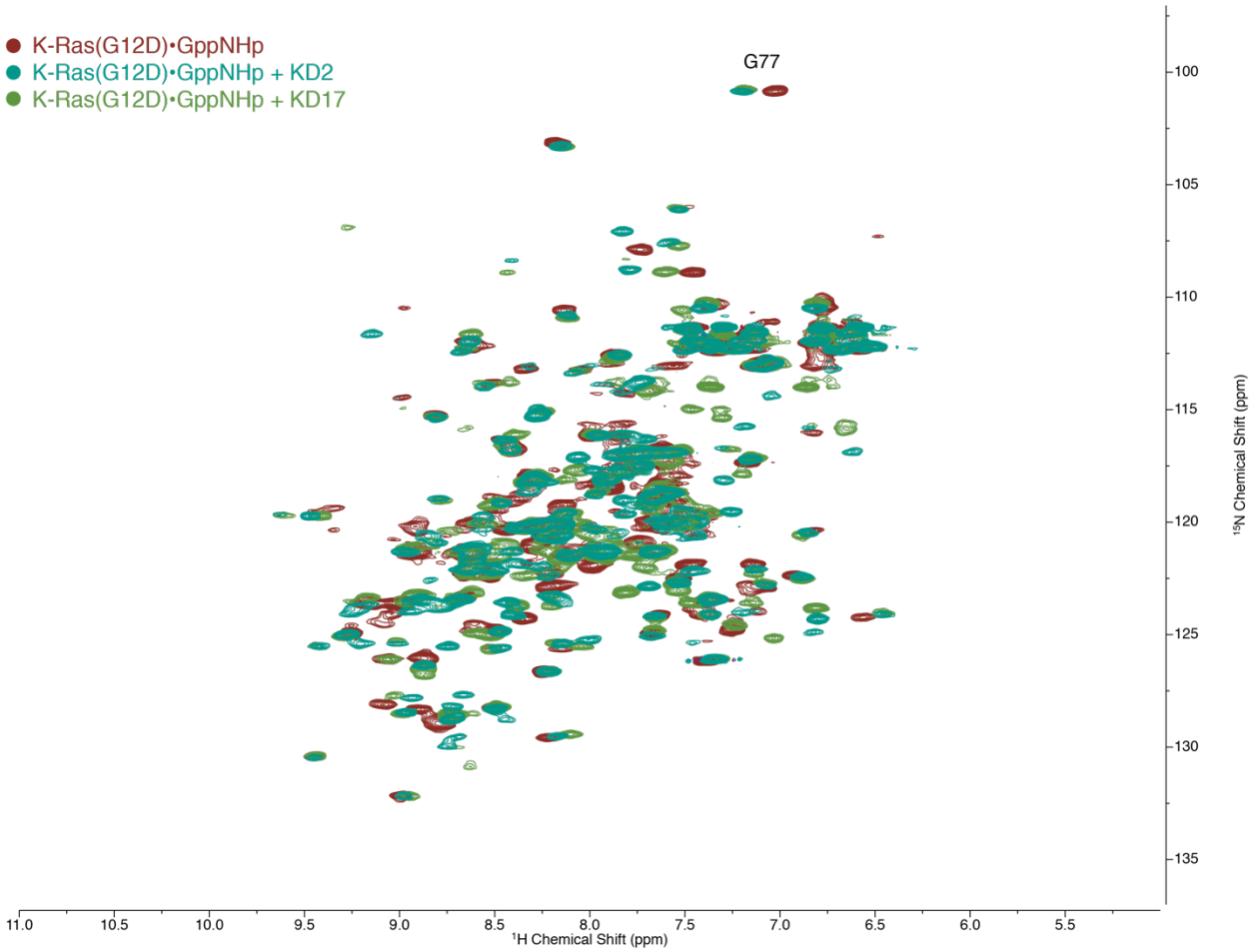

Figure S4. HSQC spectra of apo, KD2-bound, and KD17-bound K-Ras(G12D)•GppNHp showing global chemical shift perturbation upon ligand binding.

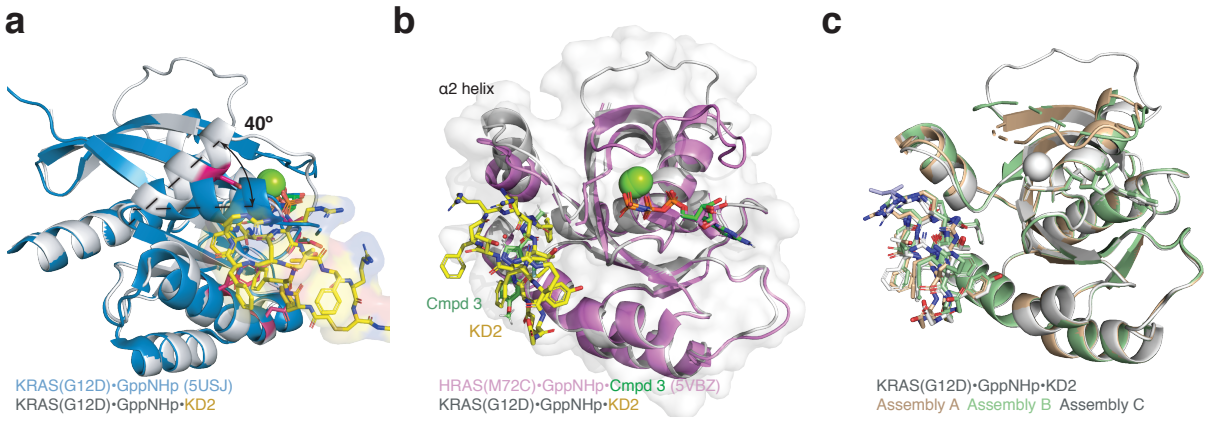

Figure S5. (Related to Figure 3). Additional views of the KD2•KRas(G12D)•GppNHp cocrystal structure. **a**, side view of the α2 helix showing the 40º rotation upon KD2 binding. **b,** comparison of K-Ras(G12D)•GppNHp•KD2 structure with H-Ras(M72C)•GppNHp•Compound 3, the latter a previously reported ligand that binds to Ras proteins in the Switch II groove. **c**, comparison of the three biological assemblies in the cocrystal structure. The conformations of K-Ras and KD2 in these three biological assemblies were congruent in most regions except Switch I, which had low electron density and may be subject to crystal packing bias.

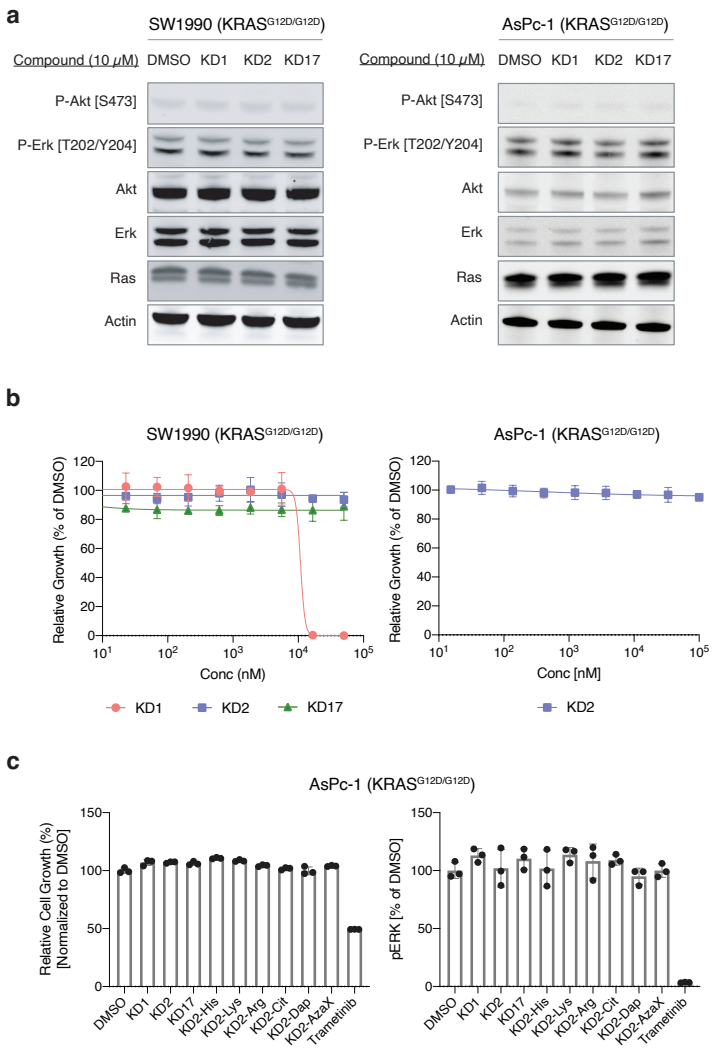

Figure S6. Cellular activity of cyclic peptides. **a**, SW1990 or AsPc-1 cells were treated with 10 μM KD1, KD2, or KD17 for 24 h and analyzed by immunoblot. **b**, SW1990 or AsPc-1 cells were treated with various concentrations of KD1, KD2, or KD17 for 72 h, and relative cell growth was determined using CellTiter Glo reagent. **c**, AsPc-1 cells were treated with 10 μM of cyclic peptides or 100 nM Trametinib. Phospho-ERK levels were assessed after 4 h using a TR-FRET based assay (signals were normalized to tubulin levels). Relative cell growth was assessed after 72 h using CellTiter Glo reagent.

a

Compound	PAMPA (10^{-6} cm/s)	Caco-2		
		A-B (10^{-6} cm/s)	B-A (10^{-6} cm/s)	Efflux ratio (B-A/A-B)
KD1	<0.001	<0.1	<0.1	NA
KD2	0.006	<0.1	0.03	>0.5
KD17	0.001	<0.6	<0.2	NA

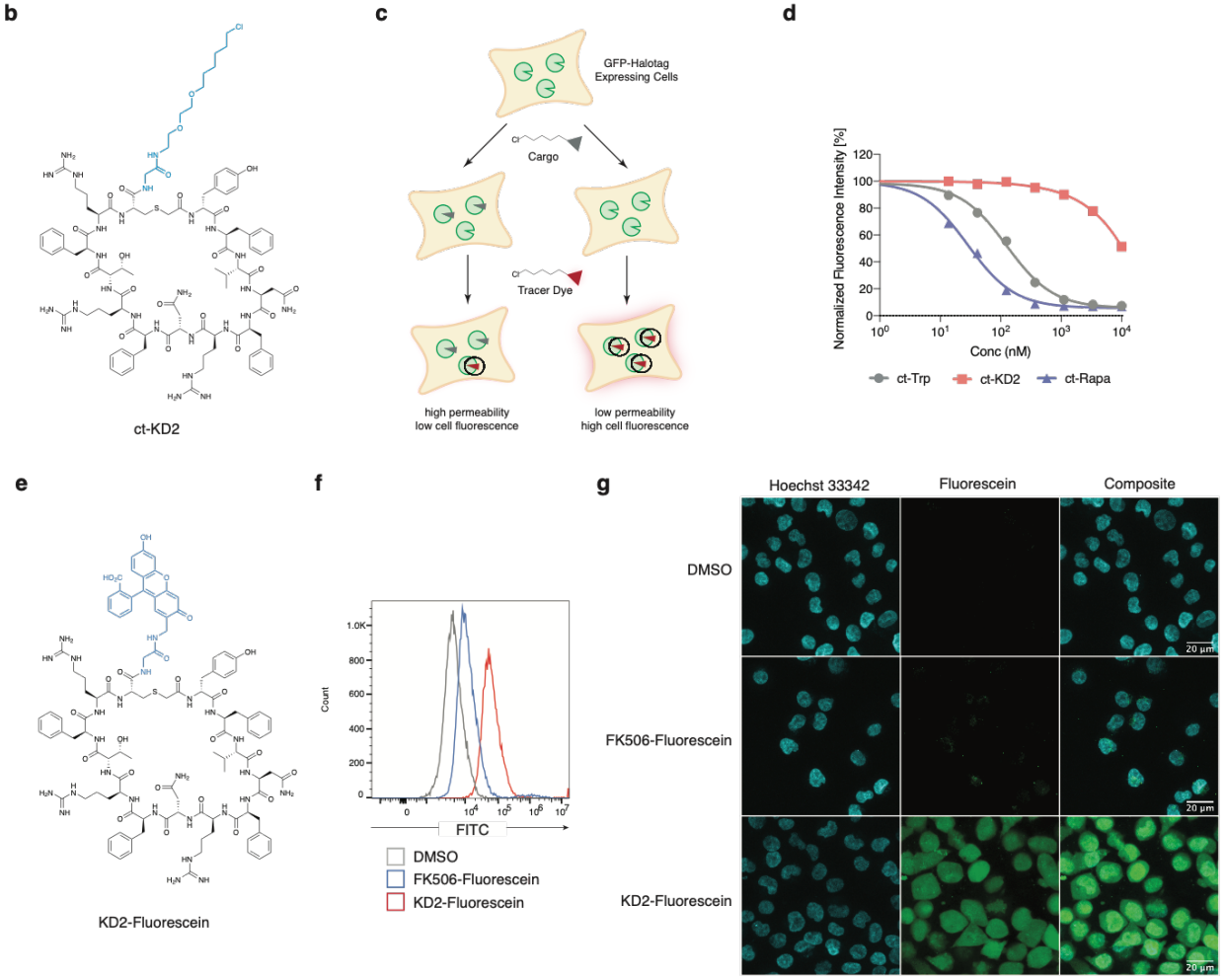

Figure S7. Cell permeability of cyclic peptides. **a**, permeability of KD1, KD2, and KD17 assessed in passive artificial membrane permeability assay (PAMPA) and Caco-2 permeability assay. structure of KD2-Fluorescein. **b**, structure of ct-KD2. **c**, graphical illustration of the chloroalkane penetration assay (CAPA). **d**, assessment of the permeability of ct-KD2 using the CAPA assay, with ct-rapamycin (ct-Rapa) as a cell permeable positive control. **e**, structure of KD2-Fluorescein. **f**, flow cytometry analysis of AsPc-1 cells treated with 10 μM FK506-fluorescein or 10 μm KD2-fluorescein for 1 h. **g**, confocal microscopy of live AsPc-1 cells treated with 10 μM FK506-Fluorescein or 10 μM KD2-Fluorescein for 1 h. Images were capture at a single z-section due to significant photobleaching of fluorescein.

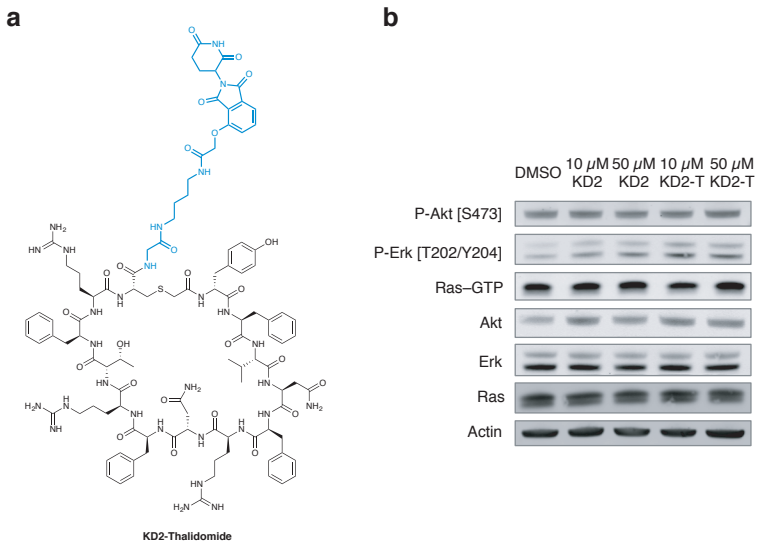

Figure S8. A KD2-Thalidomide derivative failed to induce Ras degradation. a, structure of KD2-Thalidomide. b, SW1990 cells were treated with various concentrations of KD2 or KD2-Thalidomide (KD2-T) for 24 h and analyzed by immunoblot. See the following section for an additional discussion on cellular activity.

Table S1. Data collection and refinement statistics.

	K-Ras(G12D)•KD2
Data Collection	
Space group	P 21 21 21
Cell Dimensions	
a, b, c (Å)	72.437, 79.155, 90.982
α, β, γ (º)	90, 90, 90
Resolution (Å)	50.00-1.60 (1.63-1.60)
Total reflections	69379
Unique reflections	69342
Redundancy	9.6 (7.7)
Completeness (%)	99.9 (100)
I/σ	20.1 (1.6)
R_{merge}	0.122 (0.921)
R_{meas}	0.116 (0.804)
R_{pim}	0.037 (0.286)
$CC_{1/2}$	0.998 (0.866)
*CC**	1.000 (0.963)
Refinement	
Resolution range (Å)	34.73 - 1.601 (1.659 - 1.601)
Reflections used in refinement	66446 (4750)
Reflections used for R-free	3261 (234)
R_{work}	0.1839 (0.1997)
R_{free}	0.2137 (0.2362)
Number of non-hydrogen atoms	5007
macromolecules	4334
ligands	99
solvent	574
Protein residues	539
RMS(bonds)	0.007
RMS(angles)	1.18
Ramachandran favored (%)	98.05
Ramachandran allowed (%)	1.95
Ramachandran outliers (%)	0.00
Rotamer outliers (%)	0.21
Clashscore	3.33
Average B-factor	19.61
macromolecules	18.46
ligands	12.72
solvent	29.47

* Statistics for the highest-resolution shell are shown in parentheses.

Additional Discussion on the Cellular Activity of Cyclic Peptides

We studied the cellular activity of these cyclic peptides in SW1990 and AsPc-1, cell lines with homozygous G12D mutation at the *KRAS* locus. Treatment of cells with 10 μM KD1, KD2, KD17 for 24 h did not change p-Akt or p-Erk levels (Figure S6a). KD2 also did not affect the growth of either cell lines (Figure S6b). Asking whether the KD2 analogs may have improved cellular activity, we tested an expanded set of compounds on AsPc-1 cells at 10 μM (with the MEK inhibitor trametinib as positive control), monitoring p-Erk levels after 24 h and cell growth after 72 h (Figure S6c). Under these conditions, none of these cyclic peptides led to significant reduction of p-ERK level or cell growth. To understand the discrepancy between biochemical inhibitory activity and the lack of effect on K-Ras signaling output, we asked whether these peptides entered cells. We utilized the chloroalkane cell penetration assay (CAPA)[1], which employs a cell line expressing HaloTag proteins on the outer membrane of mitochondria and monitors the cellular intake of chloroalkyl-tagged (ct) cargo compounds by quantifying the remaining unreacted HaloTag protein after exposure of cells to ct-cargo for a fixed amount of time (Figure S7b-d). Whereas two control compounds, ct-tryptophan (ct-W) and ct-rapamycin (ct-Rapa), were shown to be highly cell permeable (CP_{50} = 125 nM and 28.5 nM, respectively), ct-KD2 did not readily enter cells under the assay conditions (CP_{50} > 10 μM). Consistent with this result, we also observed low permeability of these cyclic peptides in both parallel artificial membrane permeability assay (PAMPA) and Caco-2 monolayers permeability assay (Figure S7a). Lastly, we synthesized a fluorescent derivative of KD2 (KD2-Fluorescein) and used it as a surrogate to monitor the cellular retention and localization of KD2 despite known challenges with fluorophore-conjugated compounds[2–4]. In contrast to the CAPA, PAMPA, and Caco-2 results, we observed strong staining of AsPc-1 cells by KD2-Fluorescein (Figure S7e-g). Though the additional fluorescein group may have altered the properties of KD2, the conflicting data alerted us from drawing conclusions on the cell permeability of this cyclic peptide. Despite this, we considered the possibility of using KD2 derivatives as proteolysis-targeting chimeras (PROTACs), as this class of compounds have a catalytic mechanism of action[5] and may be less restricted by low cellular permeability[6]. We synthesized KD2-thalidomide and used it to treat SW1990 cells at various concentrations. However, under no conditions was reduction of Ras protein level observed (Figure S8). Treatment with either KD2 or KD2-thalidomide also did not alter the level of Ras-GTP inside the cell. While this lack of activity could likely be ascribed to the low cell permeability of KD2 analogs, recent research has suggested that other factors (e.g. unavailability of accessible lysine on K-Ras, the identity and subcellular localization of E3 ligases, etc.) may prevent effective degradation of K-Ras[7,8]. Together, these results suggest that cell permeability is a key factor limiting the cellular activity of KD2, and improving permeability should be a critical task in future compound optimization.

Safety Notes

All experiments were performed with standard personal protective equipment (PPE). All chemical syntheses were performed in ventilated fume hoods operating at a face velocity of 90 fpm. Handling of Biosafety Level 2 materials (HeLa cells in this work) was performed according to UCSF Office of Environment, Health and Safety standards. No unexpected or unusually high safety hazards were encountered.

Cyclic Peptide Selection

Selection

Selections were performed with a thioether-macrocyclic peptide library against GppNHp-bound K-Ras(G12D/T35S), using the GDP-bound K-Ras(G12D/T35S) as the negative selection (Figure 1). Thioether-macrocyclic peptide libraries were constructed with N-chloroacetyl-D-tyrosine (ClAc^{D}Tyr) as an initiator by using the flexible *in vitro* translation (FIT) system[9]. The mRNA libraries, ClAc^{D}Tyr-tRNA$^{fMet}_{CAU}$ were prepared as reported[10–14]. The mRNA library corresponding for the thioether-macrocyclic peptide library was designed to have an AUG initiator codon to incorporate N-chloroacetyl-D-tyrosine (ClAc^{D}Tyr)[9], followed by 8–12 NNK random codons (N=G, C, A or U; K=G or U) to code for random proteinogenic amino acids, and then a fixed downstream UGC codon to for Cys. After *in vitro* translation, a thioether bond formed spontaneously between the N-terminal ClAc group of the initiator ^{D}Tyr residue and the sulfhydryl group of a downstream Cys residue.

In the first round of selection, the initial cyclic peptide library was formed by adding puromycin ligated mRNA library (225 pmol) to a 150 µL scale flexible *in vitro* translation system, in the presence of 30 µM of ClAc^{D}Tyr-tRNA$^{fMet}_{CAU}$. The translation was performed at 37 °C for 30 min, followed by an extra incubation at 25 °C for 12 min. After an addition of 15 µL of 200 mM EDTA (pH 8.0) solution, the reaction solution was incubated at 37 °C for 30 min to facilitate cyclization. Then the library was reverse-transcribed by M-MLV reverse transcriptase at 42 °C for 1 h and subject to pre-washed Sephadex G-25 columns to remove salts. The desalted solution of peptide–mRNA/cDNA was applied to GppNHp-bound K-Ras(G12D/T35S) immobilized Dynabeads M280 streptavidin magnetic beads and rotated at 4 °C for 1 h in selection buffer (25 mM HEPES pH 7.5, 150 mM NaCl, 1 mM $MgCl_2$ and 0.05% Tween 20) containing 0.5 mM GppNHp and 0.1% acetylated BSA. Bead amounts were chosen so that the final concentration of GppNHp-bound K-Ras was 200 nM. This process is referred to as positive selection. The selected peptide–mRNA/cDNAs were isolated from the beads by incubating in 1xPCR reaction buffer heated at 95 °C for 5 min. The amount of eluted cDNAs was measured by quantitative PCR (Roche LightCycler 96). The remaining cDNAs were amplified by PCR, purified and transcribed into mRNAs as a library for the next round of selection.

In each subsequent rounds of selection, ligated mRNA from the previous round (7.5 pmol) was added to a 5 µL scale reprogrammed *in vitro* translation system. This was incubated at 37 °C for 30 min and at 25 °C for 12 min. Then 1 µL of 100 mM EDTA (pH 8.0) was added and incubated at 37 °C for 30 min. After reverse transcription and salt removal using pre-washed Sephadex G-25 columns, negative selections were performed by adding the desalted solution of peptide–mRNA/cDNA to GDP-bound K-Ras(G12D/T35S) immobilized Dynabeads M280 streptavidin magnetic beads and rotating at 4 °C for 30 min in selection buffer containing 0.1% acetylated BSA. This process was repeated several times by adding the supernatant to fresh beads immobilized with GDP-bound K-Ras(G12D/T35S). The supernatant from the last negative selection was then added to beads immobilized with GppNHp-bound K-Ras(G12D/T35S) (final conc. 200nM), and rotated at 4 °C for 30 min in selection buffer containing 0.5mM GppNHp and 0.1% acetylated BSA. As described in the first round of selection, the cDNA was quantified with qPCR, amplified with PCR, transcribed and ligated to puromycin. The subsequent selection was repeated for several rounds until a significant enrichment of cDNA was observed for GppNHp-bound K-Ras(G12D/T35S). The recovered cDNA was then identified by Miseq sequencing (Illumina).

Comparison selection

In comparison selections, ligated mRNA (7.5 pmol) from last round of selection was added to a 5 µL scale reprogrammed *in vitro* translation system. After translation, cyclization, reverse transcription and salt-removal with Sephadex G-25 columns, the desalted solution of peptide–mRNA/cDNA library was split equally into three fractions, and three paralleled selections were performed with the same amount of blank, GDP-bound K-Ras(G12D/T35S) or GppNHp-bound K-Ras(G12D/T35S) immobilized Dynabeads M280 streptavidin magnetic beads. For each of the paralleled selections, the beads were rotated at 4 °C for 30 min and washed three times with selection buffer. The remaining cDNAs were then eluted from the beads, quantified by qPCR, and analyzed by Miseq sequencing. Finally, the identified sequences were compared after normalization of the Miseq abundance with its qPCR read for each paralleled selection.

Cyclic Peptide Synthesis

General Workflow

Linear peptide precursors with 2-chloroacetylated N-termini were synthesized on NovaPEG Rink-Amide resin using standard Fmoc solid-phase synthesis technology. After cleavage of the peptides from the resin, macrocyclization (S_N2 between cysteine and chloroacetamide) was performed in solution under basic conditions, and the product was purified by preparative HPLC. Detailed protocols are provided below.

Resin preparation

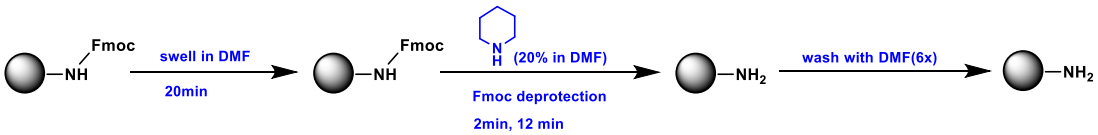

57 mg NovaPEG Rink-Amide resin (0.44 mmol/g, 25 μmol) was swelled with 4mL of DMF for at least 20 min. The resin was washed three times with DMF (4 mL each wash).
To remove the Fmoc group, 4 mL 20% piperidine (in DMF) was added to the resin and the mixture was rotated at 23 ºC for 2+12 min. The resin was washed sequentially with DMF (3 x 4 mL), DCM (3 x 4 mL) and DMF (3 x 4 mL).

Amino Acid Coupling

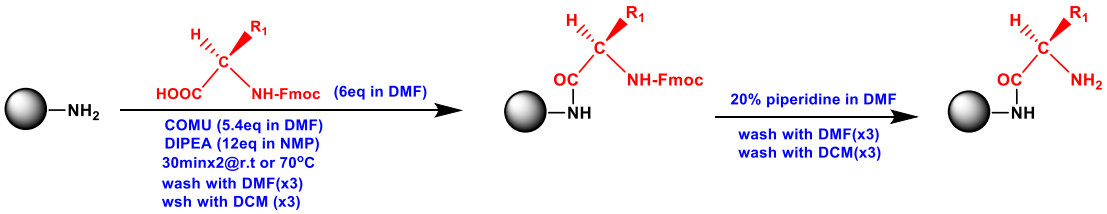

For each amino acid to be coupled to the polypeptide, a mixture of Fmoc-amino acid (600 μL of 0.5 M solution in DMF, 300 μmol), COMU (600 μL of 0.45 M solution in DMF, 270 μmol) and DIPEA (300 μL of 2.0 M solution in NMP, 600 μmol) was added to the resin and the mixture was vigorously shaken for 1 h. The resin was washed sequentially with DMF (3 x 4 mL) and DCM (3 x 4 mL). A chloranil test was performed to confirm complete coupling (a few resin beads mixed with 5 μL 2% acetaldehyde/DMF and 5 μL 2% chloranil/DMF; coupling is complete if resin is orange/yellow, incomplete if resin is blue/green/black). If coupling was incomplete, an additional round of coupling was performed using identical amounts of reagents. When coupling was complete, 4 mL of 20% piperidine (in DMF) was added and the mixture was rotated for 2 + 12 min to remove the Fmoc group. The resin was washed sequentially with DMF (3 x 4 mL), DCM (3 x 4 mL) and DMF (3 x 4 mL).
Note: In certain cases, Fmoc deprotection was performed with 4 mL 40% 4-methylpiperidine in DMF in lieu of 20% piperidine.

N-terminal capping with chloroacetamide

N-hydroxylsuccinmide chloroacetate (2 mL of 0.2 M solution in NMP) was added to peptide-conjugated resin and the mixture was rotated at 23 ºC for 1 h. A few resin beads were taken for a TNBS test. Briefly, the beads were mixed with 5 μL of 10% DIPEA/DMF

+ 5 µL 1% 2,4,6-trinitrobenzenesulfonic acid (TNBS)/DMF and incubated at 23 ºC for 10 min. Capping is complete if beads are colorless, but not if they are yellow/orange. The resin was washed by DMF (5 x 4 mL) followed by DCM (5 x 4 mL) and dried under reduced pressure overnight.

Deprotection and Cleavage

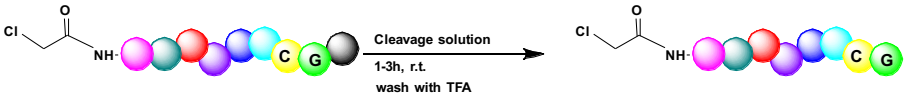

A cleavage solution was prepared as follows, chilled on ice and added to vacuum-dried resin (2 mL/25 µmol resin). The mixture was incubated on ice for 10 min, then at 23 ºC for 3 h with gentle rotation. The supernatant was filtered into a 15 mL tube, and the resin was washed with trifluoroacetic acid (3 x 1 mL). The filtrates were combined. The bulk of TFA was removed under reduced pressure on a centrifugal evaporator to ~ 1 mL volume. 20 mL ice-cold ether was added to the residue, giving rise to a white suspension, which was kept at –20 ºC for 1 h. The precipitated peptide was pelleted by centrifugation and the supernatant was discarded. The pellet was washed with diethyl ether (5 x 5 mL) by resuspension and re-pelleting, then dried under vacuum.

Cleavage solution (25 µmol scale)	TFA (trifluoroacetic acid)	1850 µL
	dH_2O	50 µL
	TIS (triisopropyl silane)	50 µL
	EDT (ethane dithiol)	50 µL
Total		2000 µL

Cyclization

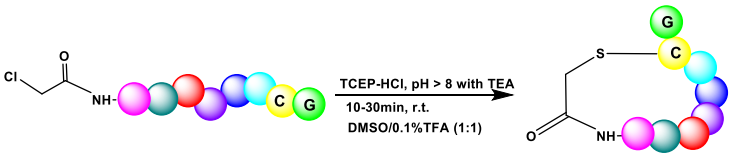

The precipitated peptide was dissolved in 5 mL DMSO. TCEP (200 µL of 500 mM solution in water) and triethylamine (100 µL) were added sequentially. The pH of the mixture should be 8. If not, adjust pH to 8 with additional triethylamine. The mixture was incubated at 23 ºC. Reaction progress was monitored by LC-MS every hour. When cyclization was complete, trifluoroacetic acid (60 µL) was added to the reaction mixture to quench the reaction. The mixture was diluted with 5 mL 0.1% TFA/water and filtered through a 0.45-µm PTFE filter. The filtered solution was purified by preparative reverse-phase HPLC (Waters XBridge C18 column 5 µm particle size 30 x 250 mm, 10–70% acetonitrile–water + 0.1% formic acid, 40 min, 20 mL/min). Product-containing fractions were concentrated under reduced pressure and lyophilized to afford the product peptide as a white powder. The counter ion was exchanged from formate to chloride by repeated

(three times) dissolution of the peptide in 5 mM HCl in 50% acetonitrile/water and removal of solvent under vacuum.

Synthesis of C-terminally Modified Cyclic Peptides (ct-KD2 and KD2-thalidomide)

To prepare C-terminally modified cyclic peptides, the parent cyclic peptide (KD2) was prepared on Wang resin in lieu of Rink resin to afford the cyclic peptide with free carboxylic acid on the C-terminus (KD2-CO_2H). KD2-CO_2H (5 µmol) was dried by azeotropic distillation from of a suspension in benzene (three times), then was dissolved in DMF (100 µL). Amine coupling partner (100 µmol) was added as a solution in DMF (100 µL) to a solution of KD2-CO_2H (5 µmol) in DMF (100 µL). DIPEA (100 µL of 2.0 M solution in DMF, 200 µmol) and HATU (100 µL of 1.0 M solution in DMF, 100 µmol) were added sequentially, the reaction mixture was incubated at 23 ºC, and the reaction progress was monitored by LC-MS. Typically, the reaction did not achieve completion and the reaction was terminated after 16 h. The reaction mixture was diluted with 50% acetonitrile–water + 0.1% formic acid to a volume to 5.0 mL, filtered through a 0.45-µm PTFE filter. The filtered solution was purified by preparative reverse-phase HPLC (Waters XBridge C18 column 5 µm particle size 30 x 250 mm, 10–70% acetonitrile–water + 0.1% formic acid, 40 min, 20 mL/min). Product-containing fractions were concentrated under reduced pressure and lyophilized to afford the product peptide as a white powder. The counterion was exchanged from formate to chloride by repeated (three times) dissolution of the peptide in 5 mM HCl in 50% acetonitrile/water and removal of solvent under vacuum.

Synthesis of Thr10 variants of KD2

Thr10 variants were prepared following the general synthesis protocol using appropriate Fmoc-protected amino acids.
For the synthesis KD2-AzaX, Fmoc-L-azidoalanine was used in lieu of Fmoc-L-threonine at position 10. All Fmoc deprotections were performed with 4-methylpiperidine/DMF.

Protein Expression and Purification

K-Ras(G12D) CysLight

K-Ras(G12D) CysLight (for crystallization only) was expressed and purified following previously reported protocols.[15,16]

Biotinylated K-Ras Proteins

pET-Duet plasmids encoding BirA biotin-protein ligase and His-Avi-TEV-tagged K-Ras proteins were constructed using standard molecular biology techniques. Biotinylated K-Ras proteins were produced in BL21(DE3) *E. coli* strain. Briefly, chemically competent BL21(DE3) cells were transformed with the corresponding pET-Duet plasmid and grown on LB agar plates containing 100 μg/mL carbenicillin. A single colony was used to inoculate a culture at 37 ºC, 220 rpm in terrific broth containing 100 μg/mL carbenicillin. When the optical density reached 0.6, the culture temperature was reduced to 20 ºC, and protein expression was induced by the addition of IPTG to 1 mM and Biotin to 5 μM. After 16 h at 20 ºC, the cells were pelleted by centrifugation (6,500 x g, 10 min) and lysed in lysis buffer [20 mM Tris 8.0, 500 mM NaCl, 5 mM imidazole] with a high-pressure homogenizer (Microfluidics, Westwood, MA). The lysate was clarified by high-speed centrifugation (19,000 x g, 15 min) and the supernatant was used in subsequent purification by immobilized metal affinity chromatography (IMAC). His-Avi-TEV tagged K-Ras protein was captured with Co-TALON resin (Clonetech, Takara Bio USA, 2 mL slurry/liter culture) at 4 ºC for 1 h with constant end-to-end mixing. The loaded beads were then washed with lysis buffer (50 mL/liter culture) and the protein was eluted with elution buffer [20 mM Tris 8.0, 500 mM NaCl, 300 mM imidazole]. The protein was further purified with anion exchange chromatography (HiTrapQ column, GE Healthcare Life Sciences) using a NaCl gradient of 50 mM to 500 mM in 20 mM Tris 8.0. Nucleotide loading was performed by mixing the ion exchange-purified protein with an excess of GDP (5 mg/liter culture) or GppNHp (5 mg/liter culture) and 5 mM EDTA at 23 ºC for 30 min. The reaction was stopped by the addition of $MgCl_2$ to 10 mM. For GppNHp, an additional calf intestine phosphatase treatment was performed as follows to ensure high homogeneity of the loaded nucleotide. The protein buffer was exchanged into Phosphatase Buffer [32 mM Tris 8.0, 200 mM ammonium sulfate, 0.1 mM $ZnCl_2$] with a HiTrap Desalting Column (GE Healthcare Life Sciences). To the buffer-exchanged protein solutions, GppNHp was added to 5 mg/mL, and Calf Intestine Phosphatase (NEB) was added to 10 U/mL. The reaction mixture was incubated on ice for 1 h, and $MgCl_2$ was added to a final concentration of 20 mM. After nucleotide loading, the protein was concentrated using an 10K MWCO centrifugal concentrator (Amicon-15, Millipore) to 20 mg/mL and purified by size exclusion chromatography on a Superdex 75 10/300 GL column (GE Healthcare Life Sciences). Fractions containing pure biotinylated Ras protein were pooled and concentrated to 20 mg/mL and stored at –78 ºC. In our hands, this protocol gives a typical yield of 5-15 mg/liter culture.

GST-Raf1-RBD and Sos^{cat}

The GST-tagged RBD domain of Raf1 (residues 1-149, GST-Raf1-RBD) was expressed and purified following a published protocol. [17]

The catalytic domain of Sos (residues 466-1049, Sos^{cat}) was expressed and purified following a published protocol.[18]

Other Proteins

GST-tagged full-length B-Raf protein (GST-BRAF) was purchased from MRC PPU (University of Dundee).

Cell Culture

SW1990 cells were obtained from ATCC and maintained in DMEM (Gibco) + 10% heat-inactivated FBS (Axenia Biologix) supplemented with penicillin and streptomycin (Gibco). HeLa cells stably expressing the HaloTag-GFP-Mito construct was a gift from Joshua Kritzer. When indicated, cells were treated with drugs at 60-80% confluency at a final DMSO concentration of 1%. At the end of treatment period, cells were placed on ice and washed once with PBS. The cells were scraped with a spatula, pelleted by centrifugation (500 x g, 5 min) and lysed in RIPA buffer supplemented with protease and phosphatase inhibitors (cOmplete and phosSTOP, Roche) on ice for 10 min. Lysates were clarified by high-speed centrifugation. Concentrations of lysates were determined with protein BCA assay (Thermo Fisher) and adjusted to 2 mg/mL with additional RIPA buffer. Samples were mixed with 5x SDS Loading Dye and heated at 95 ºC for 5 min.

Gel Electrophoresis and Western Blot

Unless otherwise noted, SDS-PAGE was run with Novex 4–12% Bis-Tris gel (Invitrogen) in MES running buffer (Invitrogen) at 200V for 40 min following the manufacturer's instructions. Protein bands were transferred onto 0.45-µm nitrocellulose membranes (Bio-Rad) using a wet-tank transfer apparatus (Bio-Rad Criterion Blotter) in 1x TOWBIN buffer with 10% methanol at 75V for 45 min. Membranes were blocked in 5% BSA–TBST for 1 h at 23 ºC. Primary antibody binding was performed with the indicated antibodies diluted in 5% BSA–TBST at 4 ºC for at l east 16 h. After washing the membrane three times with TBST (5 min each wash), secondary antibodies (goat anti-rabbit IgG-IRDye 800 and goat anti-mouse IgG-IRDye 680, Li-COR) were added as solutions in 5% skim milk–TBST at the dilutions recommended by the manufacturer. Secondary antibody binding was allowed to proceed for 1 h at 23 ºC. The membrane was washed three times with TBST (5 min each wash) and imaged on a Li-COR Odyssey fluorescence imager.

Biolayer Interferometry

Biolayer interferometry experiments were performed on a Octet Red 384 instrument (ForteBio). Biotinylated Avi-tagged K-Ras(G12D)•GppNHp protein (1 µM) was

immobilized on Streptavidin Sensor Tips (ForteBio) to a binding level of 2.0 nm. The sensors were then blocked with 10 μM Biotin. For reference sensors, 1 μM Biotin was used in lieu of the K-Ras protein. Association and dissociation curves were acquired by dipping the sensors in cyclic peptide solutions with the platform shaking at 1000 rpm. The following acquisition times were used: baseline – 60 s, association – 600 s, dissociation – 600 s. The buffers for all reagents was BLI Buffer-GppNHp, and the DMSO concentration in all cyclic peptide solutions was 0.1%.

For data analysis, signals from reference sensors (no K-Ras) were subtracted from the corresponding K-Ras-loaded sensors for each concentration point. The subtracted signals were then referenced to DMSO control for each cyclic peptide. Dissociation constants were determined by plotting steady-state binding level (averaged signal between 590 s and 595 s) against cyclic peptide concentration and fitting the curve to a one-site saturation binding model:

$$S = Smax * [Peptide] / (Kd + [Peptide])$$

Surface Plasmon Resonance

Surface plasmon resonance experiments were performed on a Biacore T200 instrument (GE Healthcare). K-Ras(G12D)•GppNHp protein was immobilized on CM5 Series S Chip (GE Healthcare) using a two-step procedure. Neutravidin was covalently coupled to the CM5 chip surface by sequentially flowing the following solutions over the chip:

1. A mixture of EDC (0.2 M) and NHS (0.05 M) in water, 20 μL/min, 500 s;
2. Neutravidin (50 μg/mL in Na-acetate pH 4.6), 20 μL/min, 150 s;
3. Ethanolamine•HCl (1.0 M, pH 8.5), 200 s.

Biotinylated Avi-tagged K-Ras(G12D)•GppNHp protein (1 μM in SPR Buffer-GppNHp) was captured on the chip surface by sequentially flowing the following solutions over the chip:

1. Biotinylated Avi-tagged K-Ras(G12D)•GppNHp protein (1 μM), 10 μL/min, 305 s;
2. Biotin (10 μM), 10 μL/min, 305 s.

For reference channels, 1 μM Biotin was used in lieu of the K-Ras protein. In general, this immobilization protocol gives an immobilization level of about 1000 RU.

Association and dissociation curves were acquired by running cyclic peptide solutions over the chip surface (30 μL/min, 150 s association, 450 s dissociation) with DMSO correction samples every 18 cycles. Except when noted, the buffers for all reagents was SPR Buffer-GppNHp, and the DMSO concentration in all cyclic peptide solutions was 0.1%.

For data analysis, signals from reference channels (no K-Ras) were subtracted from the corresponding K-Ras-loaded channels for each concentration point. The subtracted signals were then referenced to DMSO control for each cyclic peptide.

Isothermal Titration Calorimetry

Isothermal Titration Calorimetry experiments were performed on a MicroCal ITC200 instrument (GE Healthcare). K-Ras(G12D)•GppNHp or K-Ras(G12D)•GDP proteins were prepared in 2% DMSO in PBS-Mg at 40 μM. KD2 was prepared as a solution in the same buffer at 400 μM. Titration was performed at 2.0 μL/injection and 2 min equilibration time between injections, for a total of 19 injections. Data analysis was performed with the MicroCal ITC Data Analysis software provided by the manufacturer by fitting the data to a one-site binding model.

Differential Scanning Fluorimetry

The protein of interest was diluted with SEC Buffer [20 mM HEPES 7.5, 150 mM NaCl, 1 mM $MgCl_2$] to 8 μM and mixed with a 100x DMSO solution of the ligand of interest. When no ligand was added, DMSO was used. SYPRO Orange Dye (Invitrogen) was added as a 500x solution in DMSO to a final nominal concentration of 5x. The resulting mixture was dispensed into wells of a white 96-well PCR plate in triplicate (25 μL/well). Fluorescence was measured at 0.5-ºC temperature intervals every 30 s from 25 ºC to 95 ºC on a Bio-Rad CFX96 qPCR system using the FRET setting. Each data set was normalized to the highest fluorescence and the normalized fluorescence reading was plotted against temperature in GraphPad Prism 8.0. Tm values were determined as the temperature(s) corresponding to the maximum(ma) of the first derivative of the curve.

Sos- or EDTA-mediated Nucleotide Exchange Assay

This assay was performed as previously reported[15,19–21] with slight modifications.
BODIPY-GDP-loaded Avi-KRas(G12D) was prepared freshly as follows. To a 10 μM solution of Avi-KRas(G12D)•GDP in SEC Buffer (1 mL) was added sequentially BODIPY-GDP (5 mM, 40 μL, Thermo Fisher, final concentration 200 μM) and Na-EDTA pH 8.0 (0.5 M, 5 μL, final concentration 2.5 mM). The mixture was incubated at 23 ºC for 1 h, and a solution of $MgCl_2$ (1.0 M, 20 μL, final concentration 10 mM) was added to the reaction mixture. The protein solution was run through a PD-10 column to remove the excess nucleotide following the manufacturer's protocol. Briefly, sample (~1.0 mL) and excess buffer (1.5 mL) were loaded onto the column (equilibrated with NucEx Buffer), and desalted protein was eluted with NucEx Buffer (3.5 mL). Protein concentration was measured with Bradford assay and adjusted to 1.25 μM with NucEx Buffer.
50 μL protein solution was mixed with 0.5 μL DMSO solution of the test compound and the mixture was incubated at 23 ºC for 15 min. 12 μL of this solution (triplicate for each condition) was added to wells of a black 384-well low-volume assay plate (Corning 4514). 3 μL of either 1 mM GDP, 1 mM GDP + 5 μM Sos, or 1 mM GDP + 40 mM EDTA (all

prepared in NucEx Buffer) was added via a multichannel pipet rapidly to the wells. This should take less than 15 s to finish. The plate was immediately placed in a TECAN Spark 20M plate reader, and fluorescence for BODIPY (excitation 488 nm, emission 520 nm) was read every 30 s over 1 h. Fluorescence intensity was normalized to values at time 0 and plotted again time. Observed rate constant (k_{obs}) was derived by fitting the curve to first-order kinetic equation

$$F = (F_0 - F_\infty) \exp[-k_{obs}t] + F_\infty$$

and plotted against time.

Time-Resolved Fluorescence Resonance Energy Transfer (TR-FRET) Assay

TR-FRET assay was performed using recommended conditions from Cisbio with slight modifications. For GST-Raf1-RBD assays, biotinylated Ras proteins were diluted in TR-FRET buffer to 25 nM, and GST-Raf1-RBD was in TR-FRET buffer to 25 nM. For GST-BRAF assays, biotinylated Ras proteins were diluted in TR-FRET buffer to 250 nM and GST-BRAF was diluted to 250 nM. These concentrations were determined previously with titrations of both reagents to allow the maximal assay window. The difference between the GST-Raf1-RBD assay and GST-BRAF likely reflects the lower affinity of full length BRAF for Ras (Fisher et al. *J. Biol. Chem.* 2007, 282, 26503–26516). Anti-GST-Tb (Cisbo) was diluted to 500 ng/mL. Streptavidin-XL665 (Cisbio) was diluted to 10 µg/mL. Compounds were prepared at 5x testing concentrations in TR-FRET assay buffer (5% DMSO). For each replicate of each assay condition, 4 µL compound solution, 4 µL of diluted Ras protein, 4 µL diluted GST-Raf1-RBD or GST-BRAF was mixed in a well of a black low-volume 384-well plate (Corning 4514), and the mixture was incubated at 23 ºC for 1 h. 4 µL of Anti-GST-Tb and 4 µL of Streptavidin-XL665 were then added sequentially to each assay well, and the mixture was incubated at 23 ºC for an additional 1 h. Time-resolved fluorescence was read on a TECAN Spark 20M plate reader with the following parameters:

Lag time: 60 µs
Integration time: 500 µs
Read A: Excitation filter 320(25) nm, Emission filter 610(25) nm, Gain 130
Read B: Excitation filter 320(25) nm, Emission filter 665(8) nm, Gain 165

TR-FRET signal was calculated as the ratio fluorescence intensity [Read B]/[Read A]. The ratiometric signal was further normalized to a negative control containing GDP-bound Ras protein. Three replicates were performed for each assay condition.

Chloroalkane Cell Penetration (CAPA) Assay

This assay was performed following published protocols (Peraro et al. 2018). Briefly, Hela cells stably expressing HaloTag-GFP-Mito were were seeded in a 96-well plate the day before the experiment at a density of 4×10^4 cells per well. The day of the experiment

the media was aspirated, and 100 µL of Opti-MEM was added to the cells. Test compounds at 500x assay concentration were diluted in Opti-MEM to 5x, and serial dilutions of the peptides were performed in a separate 96-well plate (final DMSO: 1%). 25 µL of compound solution was added to each well, and the plate was incubated for 4 h at 37 °C with 5% CO_2. The contents of the wells were aspirated off, and wells were washed using fresh Opti-MEM for 15 min. The wash was aspirated off, and the cells were chased using 5 µM ct-TAMRA (Promega) for 15 min, except for the control wells, which were incubated with Opti-MEM alone. The contents of the wells were aspirated and washed with fresh Opti-MEM for 30 min. After aspiration, cells were rinsed once with phosphate-buffered saline (PBS). The cells were then trypsinized, resuspended in PBS, and analyzed using an Attune NxT flow cytometer (Thermo Fisher Scientific). Data analysis was performed on GFP positive cell population, and median fluorescence intensity (MFI) in the TAMRA channel, normalized to DMSO treatment control, was plotted against peptide concentration.

Passive Artificial Membrane Permeability Assay (PAMPA)

PAMPA assay was performed by Quintara Discovery Inc. (qdibio.com).

Caco-2 Monolayer Permeability Assay

PAMPA assay was performed by Quintara Discovery Inc. (qdibio.com).

Crystallization

GppNHp-loaded K-Ras Cyslight (G12D/C51S/C80L/C118S) purified by size exclusion chromatography was concentrated to 20 mg/mL and 100 µL protein was mixed with 5 µL 30 mM cyclic peptide solution in DMSO and 5 µL 100 mM GppNHp in SEC buffer. The mixture was incubated at 23 ºC for 24 h and centrifuged (21,000 x g, 30 min) to remove particulates. The supernatant was transferred into new tubes. For crystallization, 0.1 µL of the protein was mixed with 0.1 µL well buffer containing 0.1 M Tris 9.0, 0.2 M lithium sulfate, 30% PEG4000. Crystals were grown at 20 ºC in a 96-well plate using the hanging-drop vapor diffusion method. Maximal crystal growth was achieved after 25 days. The crystals were transferred to a cryoprotectant solution (0.1 M Tris 9.0, 0.2 M lithium sulfate, 30% PEG4000, 20% glycerol) and flash-frozen in liquid nitrogen.

X-Ray Data Collection and Structure Determination

Dataset was collected at the Advanced Light Source beamline 8.2.2 with X-ray at a wavelength of 0.999907 Å. The dataset was indexed and integrated using iMosflm (Battye et al., 2011), scaled with Scala (Evans, 2006) and solved by molecular replacement using Phaser (McCoy et al., 2007) in CCP4 software suite (Winn et al., 2011). The crystal structure of GppNHp-bound K-Ras(G12D) (PDB code: 5USJ) was used as the initial model. The structure was manually refined with Coot (Emsley et al., 2010) and PHENIX (Adams et al., 2010). Data collection and refinement statistics are listed in Table S1. In the Ramachandran plot of the final structure, 97.86% and 1.95% of the residues are in the favored regions and allowed regions, respectively. One residue, Arg41, directly adjacent to the partially disordered Switch I region (32-40), is calculated as an outlier.

Heteronuclear Single-Quantum Coherence (HSQC)

Samples of ^{15}N-labeled, GppNHp-bound K-Ras(G12D) for NMR spectroscopy were prepared as follows. A 30 µL aliquot of protein at 1.0 mM in storage buffer (40 mM HEPES pH 7.4, 150 mM NaCl, 4 mM MgCl2, 5% v/v glycerol, 7% v/v D2O) was diluted with 240 µL of buffer (40 mM HEPES pH 7.4, 150 mM NaCl, 4 mM MgCl2, 7% v/v D2O) in a 1.2 ml Eppendorf tube on ice. Then, 30 µL of either dmso-d6, or a cyclic peptide at 4.0 mM in dmso-d6 were added, the sample was mixed, and the resulting solution was transferred to a 5 mM D2O-matched Shigemi NMR tube (BMS-3). The final concentrations of protein and cyclic peptide were 100 and 400 µM, respectively.

^{1}H-^{15}N HSQC spectra (fhsqcf3gpph) were acquired on an 800 MHz Bruker Neo spectrometer at 288 K with 1024 and 512 points, 8 scans, and GARP decoupling. Chemical shifts were referenced to the HDO signal at 4.70 ppm.

Materials

Guanosine 5'-[β,γ-imido]triphosphate trisodium salt hydrate (GppNHp) and Guanosine 5'-diphosphate sodium salt were ordered from Sigma (St. Louis, MO, USA). Sephadex™ G-25 fine was ordered from GE healthcare (Uppsala, Sweden). Acetylated bovine serum albumin (nuclease and protease tested) were ordered from Nacalai Tesque, Inc. (Kyoto, Japan). M-MLV Reverse Transcriptase and RNasin Plus RNase inhibitor were obtained from Promega (Madison, WI, USA). Dynabeads M280 streptavidin was purchased from Thermo Fisher Scientific (Baltics, USA).

List of Antibodies

Target	Supplier	Identifier	Dilution
Pan-Ras	abcam	108062	1:5000
P-ERK [T202/Y204]	Cell Signaling Technology	9101	1:1000
Total ERK	Cell Signaling Technology	4695	1:1000
P-S6 [S240/S244]	Cell Signaling Technology	5364	1:2000
S6	Cell Signaling Technology	2217	1:1000
P-AKT [S473]	Cell Signaling Technology	4060	1:1000
AKT	Cell Signaling Technology	2920	1:1000
Actin	Proteintech	60008-1-Ig	1:50000

List of Buffer Composition

Name	Composition
RIPA Buffer	25 mM Tris 7.4 150 mM NaCl 0.1% SDS 1% NP-40 0.5% sodium deoxycholate
Lysis Buffer	20 mM Tris 8.0 500 mM NaCl 5 mM imidazole
Elution Buffer	20 mM Tris 8.0 300 mM NaCl 300 mM imidazole
Phosphatase Buffer	32 mM Tris 8.0 200 mM ammonium sulfate 0.1 mM $ZnCl_2$
SEC Buffer	20 mM HEPES 8.0 150 mM NaCl 1 mM $MgCl_2$
NucEx Buffer	20 mM HEPES 7.5 150 mM NaCl 1 mM $MgCl_2$ 1 mM DTT
TR-FRET Buffer	20 mM HEPES 7.5 150 mM NaCl 1 mM $MgCl_2$ 0.05% Tween-20 0.1% BSA 0.5 mM DTT

BLI Buffer-GppNHp	20 mM HEPES 7.5 150 mM NaCl 1 mM MgCl2 0.05% Tween-20 0.1% BSA 10 μM GppNHp
SPR Buffer-GppNHp	20 mM HEPES 7.5 150 mM NaCl 1 mM MgCl2 0.05% Tween-20 10 μM GppNHp

List of Protein Sequences Used in This Study

Texts in red indicate the affinity tags that were cleaved during purification.

>KRAS CysLight (G12D)
MHHHHHHSSGRENLYFQGMTEYKLVVVGADGVGKSALTIQLIQNHFVDEYDPTIEDSYRKQVVIDGETSL
LDILDTAGQEEYSAMRDQYMRTGEGFLLVFAINNTKSFEDIHHYREQIKRVKDSEDVPMVLVGNKSDLPS
RTVDTKQAQDLARSYGIPFIETSAKTRQGVDDAFYTLVREIRKHKEK

>His-Avi-TEV-KRAS (G12D)
MGSSHHHHHHSGMSGLNDIFEAQKIEWHESSGENLYFQGMTEYKLVVVGADGVGKSALTIQLIQNHFVDE
YDPTIEDSYRKQVVIDGETCLLDILDTAGQEEYSAMRDQYMRTGEGFLCVFAINNTKSFEDIHHYREQIK
RVKDSEDVPMVLVGNKCDLPSRTVDTKQAQDLARSYGIPFIETSAKTRQGVDDAFYTLVREIRKHKEK

>His-Avi-TEV-KRAS (wildtype)
MGSSHHHHHHSGMSGLNDIFEAQKIEWHESSGENLYFQGMTEYKLVVVGAGGVGKSALTIQLIQNHFVDE
YDPTIEDSYRKQVVIDGETCLLDILDTAGQEEYSAMRDQYMRTGEGFLCVFAINNTKSFEDIHHYREQIK
RVKDSEDVPMVLVGNKCDLPSRTVDTKQAQDLARSYGIPFIETSAKTRQGVDDAFYTLVREIRKHKEK

>GST-Raf1-RBD
MSPILGYWKIKGLVQPTRLLLEYLEEKYEEHLYERDEGDKWRNKKFELGLEFPNLPYYIDGDVKLTQSMA
IIRYIADKHNMLGGCPKERAEISMLEGAVLDIRYGVSRIAYSKDFETLKVDFLSKLPEMLKMFEDRLCHK
TYLNGDHVTHPDFMLYDALDVVLYMDPMCLDAFPKLVCFKKRIEAIPQIDKYLKSSKYIAWPLQGWQATF
GGGDHPPKSDLVPRGSPIHIMEHIQGAWKTISNGFGFKDAVFDGSSCISPTIVQQFGYQRRASDDGKLTD
PSKTSNTIRVFLPNKQRTVVNVRNGMSLHDCLMKALKVRGLQPECCAVFRLLHEHKGKKARLDWNTDAAS
LIGEELQVDFLDHVPLTTHNFARKTFLKLGIHRD

>GST-BRAF
MSPILGYWKIKGLVQPTRLLLEYLEEKYEEHLYERDEGDKWRNKKFELGLEFPNLPYYIDGDVKLTQSMA
IIRYIADKHNMLGGCPKERAEISMLEGAVLDIRYGVSRIAYSKDFETLKVDFLSKLPEMLKMFEDRLCHK
TYLNGDHVTHPDFMLYDALDVVLYMDPMCLDAFPKLVCFKKRIEAIPQIDKYLKSSKYIAWPLQGWQATF
GGGDHPPKSDLEVLFQGPLGSPNSRVDAALSGGGGGGAEPGQALFNGDMEPEAGAGAGAAASSAADPAIP
EEVWNIKQMIKLTQEHIEALLDKFGGEHNPPSIYLEAYEEYTSKLDALQQREQQLLESLGNGTDFSVSSS
ASMDTVTSSSSSSLSVLPSSLSVFQNPTDVARSNPKSPQKPIVRVFLPNKQRTVVPARCGVTVRDSLKKA

LMMRGLIPECCAVYRIQDGEKKPIGWDTDISWLTGEELHVEVLENVPLTTHNFVRKTFFTLAFCDFCRKL
LFQGFRCQTCGYKFHQRCSTEVPLMCVNYDQLDLLFVSKFFEHHPIPQEEASLAETALTSGSSPSAPASD
SIGPQILTSPSPSKSIPIPQPFRPADEDHRNQFGQRDRSSSAPNVHINTIEPVNIDDLIRDQGFRGDGGS
TTGLSATPPASLPGSLTNVKALQKSPGPQRERKSSSSSEDRNRMKTLGRRDSSDDWEIPDGQITVGQRIG
SGSFGTVYKGKWHGDVAVKMLNVTAPTPQQLQAFKNEVGVLRKTRHVNILLFMGYSTKPQLAIVTQWCEG
SSLYHHLHIIETKFEMIKLIDIARQTAQGMDYLHAKSIIHRDLKSNNIFLHEDLTVKIGDFGLATVKSRW
SGSHQFEQLSGSILWMAPEVIRMQDKNPYSFQSDVYAFGIVLYELMTGQLPYSNINNRDQIIFMVGRGYL
SPDLSKVRSNCPKAMKRLMAECLKKKRDERPLFPQILASIELLARSLPKIHRSASEPSLNRAGFQTEDFS
LYACASPKTPIQAGGYGAFPVH

Characterization Data for Cyclic Peptides

Mass Spectrometry

Name	Sequence	m/z (calc'd for 2+)	m/z (found for 2+)
KD1	^{D}YIIVTEKFIWVHHCG	942.4856	942.4811
KD2	^{D}YFVNFRNFRTFRCG	933.4552	933.4468
KD17	^{D}YNYPYRPLELGWYCG	966.9412	966.9338
KD2-His	^{D}YFVNFRNFRHFRCG	951.9529	951.9568
KD2-Lys	^{D}YFVNFRNFRKFRCG	947.4709	947.4713
KD2-Arg	^{D}YFVNFRNFRRFRCG	961.4740	961.4735
KD2-Dap	^{D}YFVNFRNFR(Dap)FRCG	926.4474	926.4488
KD2-Cit	^{D}YFVNFRNFR(Cit)FRCG	961.9660	961.9687
KD2-AzaX	^{D}YFVNFRNFR(Pip)FRCG	967.4865	967.4877
KD2-CO_2H	^{D}YFVNFRNFRTFRCG-CO_2H	933.9472	933.9476
Ct-KD2	^{D}YFVNFRNFRTFRCG-Ct	1036.5088	1036.5116
KD2-Thal	^{D}YFVNFRNFRTFRCG-Thal	1126.0189	1126.0177

UPLC Analysis

KD1

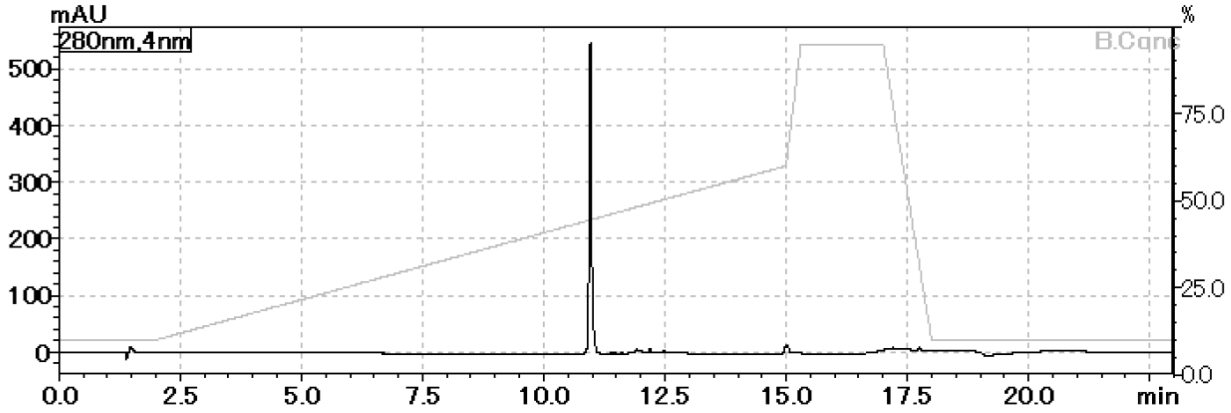

KD2

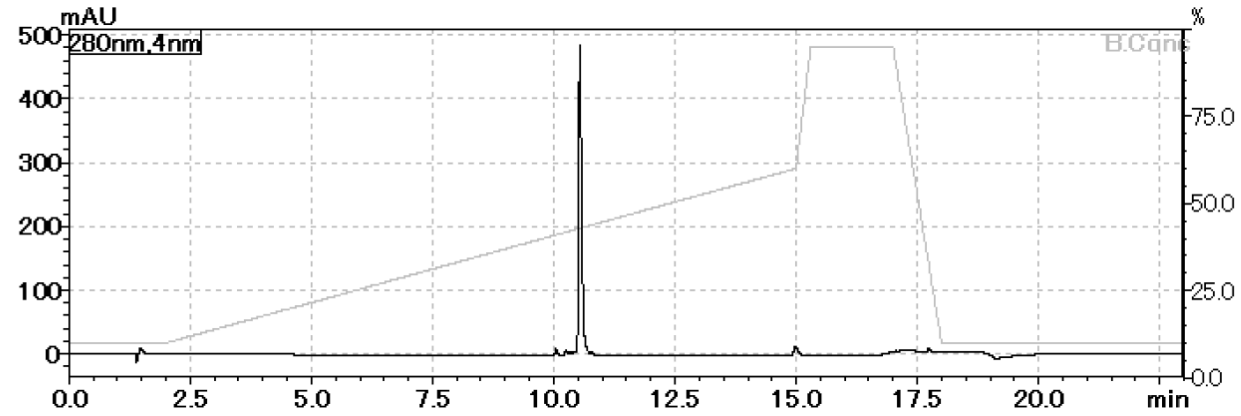
mAU
280nm,4nm
%
500
400
300
200
100
0
75.0
50.0
25.0
0.0
0.0
2.5
5.0
7.5
10.0
12.5
15.0
17.5
20.0
min

KD17

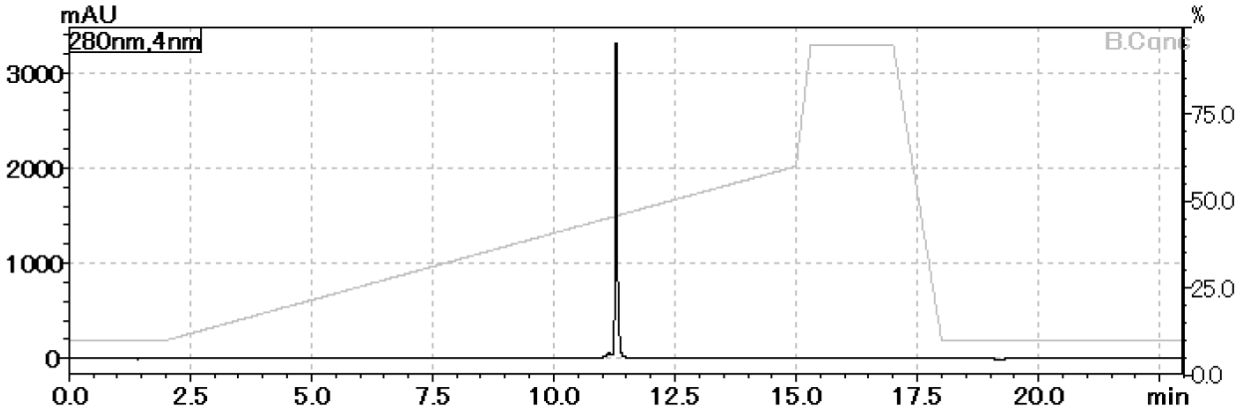
mAU
280nm,4nm
%
3000
2000
1000
0
75.0
50.0
25.0
0.0
0.0
2.5
5.0
7.5
10.0
12.5
15.0
17.5
20.0
min

References

(1) Peraro, L.; Deprey, K. L.; Moser, M. K.; Zou, Z.; Ball, H. L.; Levine, B.; Kritzer, J. A. Cell Penetration Profiling Using the Chloroalkane Penetration Assay. *J. Am. Chem. Soc.* **2018**, *140* (36), 11360–11369.

(2) Best, T. P.; Edelson, B. S.; Nickols, N. G.; Dervan, P. B. Nuclear Localization of Pyrrole-Imidazole Polyamide-Fluorescein Conjugates in Cell Culture. *Proc. Natl. Acad. Sci. U. S. A.* **2003**, *100* (21), 12063–12068.

(3) Birch, D.; Christensen, M. V.; Staerk, D.; Franzyk, H.; Nielsen, H. M. Fluorophore Labeling of a Cell-Penetrating Peptide Induces Differential Effects on Its Cellular Distribution and Affects Cell Viability. *Biochim. Biophys. Acta - Biomembr.* **2017**, *1859* (12), 2483–2494.

(4) Hedegaard, S. F.; Derbas, M. S.; Lind, T. K.; Kasimova, M. R.; Christensen, M. V.; Michaelsen, M. H.; Campbell, R. A.; Jorgensen, L.; Franzyk, H.; Cárdenas, M.; Nielsen, H. M. Fluorophore Labeling of a Cell-Penetrating Peptide Significantly Alters the Mode and Degree of Biomembrane Interaction. *Sci. Rep.* **2018**, *8* (1), 1–14.

(5) Bondeson, D. P.; Mares, A.; Smith, I. E. D.; Ko, E.; Campos, S.; Miah, A. H.; Mulholland, K. E.; Routly, N.; Buckley, D. L.; Gustafson, J. L.; Zinn, N.; Grandi, P.; Shimamura, S.; Bergamini, G.; Faelth-Savitski, M.; Bantscheff, M.; Cox, C.; Gordon, D. A.; Willard, R. R.; Flanagan, J. J.; Casillas, L. N.; Votta, B. J.; Den Besten, W.; Famm, K.; Kruidenier, L.; Carter, P. S.; Harling, J. D.; Churcher, I.; Crews, C. M. Catalytic in Vivo Protein Knockdown by Small-Molecule PROTACs. *Nat. Chem. Biol.* **2015**, *11* (8), 611–617.

(6) Foley, C. A.; Potjewyd, F.; Lamb, K. N.; James, L. I.; Frye, S. V. Assessing the Cell Permeability of Bivalent Chemical Degraders Using the Chloroalkane Penetration Assay. *ACS Chem. Biol.* **2020**, *15* (1), 290–295.

(7) Zeng, M.; Xiong, Y.; Safaee, N.; Nowak, R. P.; Donovan, K. A.; Yuan, C. J.; Nabet, B.; Gero, T. W.; Feru, F.; Li, L.; Gondi, S.; Ombelets, L. J.; Quan, C.; Jänne, P. A.; Kostic, M.; Scott, D. A.; Westover, K. D.; Fischer, E. S.; Gray, N. S. Exploring Targeted Degradation Strategy for Oncogenic KRASG12C. *Cell Chem. Biol.* **2020**, *27* (1), 19-31.e6.

(8) Bond, M. J.; Chu, L.; Nalawansha, D. A.; Li, K.; Crews, C. Targeted Degradation of Oncogenic KRASG12C by VHL-Recruiting PROTACs. *ChemRxiv* **2020**, https://doi.org/10.26434/chemrxiv.12091176.v1.

(9) Goto, Y.; Katoh, T.; Suga, H. Flexizymes for Genetic Code Reprogramming. *Nat. Protoc.* **2011**, *6* (6), 779–790.

(10) Hayashi, Y.; Morimoto, J.; Suga, H. In Vitro Selection of Anti-Akt2 Thioether-Macrocyclic Peptides Leading to Isoform-Selective Inhibitors. *ACS Chem. Biol.* **2012**, *7* (3), 607–613.

(11) Hipolito, C. J.; Tanaka, Y.; Katoh, T.; Nureki, O.; Suga, H. A Macrocyclic Peptide That Serves as a Cocrystallization Ligand and Inhibits the Function of a MATE Family Transporter. *Molecules* **2013**, *18* (9), 10514–10530.

(12) Morimoto, J.; Hayashi, Y.; Suga, H. Discovery of Macrocyclic Peptides Armed with a Mechanism-Based Warhead: Isoform-Selective Inhibition of Human Deacetylase SIRT2. *Angew. Chemie - Int. Ed.* **2012**, *51* (14), 3423–3427.

(13) Yamagata, K.; Goto, Y.; Nishimasu, H.; Morimoto, J.; Ishitani, R.; Dohmae, N.;

Takeda, N.; Nagai, R.; Komuro, I.; Suga, H.; Nureki, O. Structural Basis for Potent Inhibition of SIRT2 Deacetylase by a Macrocyclic Peptide Inducing Dynamic Structural Change. *Structure* **2014**, *22* (2), 345–352.

(14) Yamagishi, Y.; Shoji, I.; Miyagawa, S.; Kawakami, T.; Katoh, T.; Goto, Y.; Suga, H. Natural Product-like Macrocyclic N-Methyl-Peptide Inhibitors against a Ubiquitin Ligase Uncovered from a Ribosome-Expressed de Novo Library. *Chem. Biol.* **2011**, *18* (12), 1562–1570.

(15) Ostrem, J. M.; Peters, U.; Sos, M. L.; Wells, J. A.; Shokat, K. M. K-Ras(G12C) Inhibitors Allosterically Control GTP Affinity and Effector Interactions. *Nature* **2013**, *503* (7477), 548–551.

(16) Gentile, D. R.; Rathinaswamy, M. K.; Jenkins, M. L.; Moss, S. M.; Siempelkamp, B. D.; Renslo, A. R.; Burke, J. E.; Shokat, K. M. Ras Binder Induces a Modified Switch-II Pocket in GTP and GDP States. *Cell Chem. Biol.* **2017**, *24* (12), 1455-1466.e14.

(17) Brtva, T. R.; Drugan, J. K.; Ghosh, S.; Terrell, R. S.; Campbell-Burk, S.; Bell, R. M.; Der, C. J. Two Distinct Raf Domains Mediate Interaction with Ras. *J. Biol. Chem.* **1995**, *270* (17), 9809–9812.

(18) Sondermann, H.; Soisson, S. M.; Boykevisch, S.; Yang, S. S.; Bar-Sagi, D.; Kuriyan, J. Structural Analysis of Autoinhibition in the Ras Activator Son of Sevenless. *Cell* **2004**, *119* (3), 393–405.

(19) Ahmadian, M. R.; Zor, T.; Vogt, D.; Kabsch, W.; Selinger, Z.; Wittinghofer, a; Scheffzek, K. Guanosine Triphosphatase Stimulation of Oncogenic Ras Mutants. *Proc. Natl. Acad. Sci. U. S. A.* **1999**, *96* (12), 7065–7070.

(20) Huehls, A. M.; Coupet, T. A.; Sentman, C. L. Bispecific T-Cell Engagers for Cancer Immunotherapy. *Immunol. Cell Biol.* **2014**, *93* (10), 290–296.

(21) Maurer, T.; Garrenton, L. S.; Oh, A.; Pitts, K.; Anderson, D. J.; Skelton, N. J.; Fauber, B. P.; Pan, B.; Malek, S.; Stokoe, D.; Ludlam, M. J. C.; Bowman, K. K.; Wu, J.; Giannetti, A. M.; Starovasnik, M. A.; Mellman, I.; Jackson, P. K.; Rudolph, J.; Wang, W.; Fang, G. Small-Molecule Ligands Bind to a Distinct Pocket in Ras and Inhibit SOS-Mediated Nucleotide Exchange Activity. *Proc. Natl. Acad. Sci. U. S. A.* **2012**, *109* (14), 5299–5304.